

Rotating wheel filter design and optimization for a uniform depth dose distribution in heavy ion therapy^{*}

ZHOU Qing-Ming(周清明)^{1,2,3} ZHANG Hong(张红)^{1,3;1)} LI Qiang(李强)¹
WEI Li-Li(危黎黎)⁴ LIU Xin-Guo(刘新国)^{1,2} GU Meng-Xia(顾梦霞)⁵
WU Gui-Hong(吴桂红)⁶ DAI Zhong-Yin(戴中颖)^{1,2}

1 (Institute of Modern Physics, Chinese Academy of Sciences, Lanzhou 730000, China)

2 (Graduate School of Chinese Academy of Sciences, Beijing 100049, China)

3 (Key Laboratory of Heavy Ion Radiation Medicine of Gansu Province, Lanzhou 730000, China)

4 (College of Arts and Science of Jiangnan University, Wuhan 430000, China)

5 (Hubei University of Technology, Wuhan 430068, China)

6 (School of Sciences, Central South University of Forestry and Technology, Zhuzhou 412006, China)

Abstract Treatment planning of heavy-ion radiotherapy involves predictive calculation of not only the physical dose but also the biological dose in a patient body. The goal in designing beam-modulating devices for heavy ion therapy is to achieve uniform biological effects across the spread-out Bragg peak (SOBP). To achieve this, a mathematical model of Bragg peak movement is presented. The parameters of this model have been resolved with Monte Carlo method. And a rotating wheel filter is designed basing on the velocity of the Bragg peak movement.

Key words heavy ion, spread-out Bragg peak, rotating wheel filter, Monte Carlo method

PACS 87.55.N-, 45.20.dc, 02.60.Pn

1 Introduction

The main reason for the increasing interest in the use of heavy ion beam for radiotherapy is its high potential for sparing healthy tissue surrounding a tumor, which is due to its inverted depth-dose distribution presenting a Bragg peak at the end of its range. In addition, heavy ion beam shows a considerable increase in biological effectiveness in the peak^[1]. Heavy ion beam is thus a promising tool for the radiation therapy of deep-seated tumors. Pioneering work of heavy ion radiotherapy has been conducted at Lawrence Berkeley laboratory and was reviewed by Chu et al^[2].

In conventional application, heavy ion beam is spreaded laterally by scattering or wobbling method, while a uniform dose distribution in depth is achieved by an energy modulation through a modulator wheel or a ridge filter^[3, 4]. Thorough mixing of the particles with different ranges may occur through scattering in the ridge filter material and subsequent absorber, or the filter may be made to oscillate across the beam to average out any inhomogeneity^[4]. This broadening produces a fluctuation of the linear energy transfer (LET) throughout the spread-out Bragg peak (SOBP). Any variation in LET induces a fluctuation in relative biological effectiveness (RBE) as well. This phenomenon must be taken into account

Received 8 July 2008

^{*} Supported by National Natural Science Foundation of China (10675151), Key Scientific Technology Research Projects of Gansu Province (2GS052-A43-00 8-02, 2GS063-A43-012) and Scientific Technology Research Project of Lanzhou-Chinese Academy of Sciences (06-2-58)

1) E-mail: zhangh@impcas.ac.cn

in designing the SOBP in the case of modulation of high-LET heavy-ion beams^[1].

Jongen et al reported a rotating energy absorber^[5]. This device makes the Bragg peak move in the continuous velocity. But the beam penetrates the device through the diameter direction, resulting in a big space occupied in the beam direction. And they did not provide the parameter computing method of the rotating energy absorber.

In this paper, a rotating wheel filter is designed on the basis of the velocity of the Bragg peak movement, which synthesizes the advantages presented in both of the rotating, stepped absorber described by Koehler^[4] and the rotating energy absorber described by Jongen^[5]. Moreover, the designing parameter is calculated with Monte Carlo method.

2 Material and methods

2.1 Design of the wheel and its movement

The surface of the section that is penetrated by the beam can be described by the following function,

$$\begin{cases} x = r \cdot \cos(\alpha) \\ y = r \cdot \sin(\alpha) \\ z = C + C_m \cdot \int_0^t v(t) dt \end{cases},$$

$$\text{here, } t = \begin{cases} \frac{2 \cdot (\pi + \alpha)}{\pi} & \text{for } \alpha \in [-\pi, -\frac{\pi}{2}) \\ \frac{2 \cdot (-\alpha)}{\pi} & \text{for } \alpha \in [-\frac{\pi}{2}, 0) \\ \frac{2 \cdot \alpha}{\pi} & \text{for } \alpha \in [0, \frac{\pi}{2}) \\ \frac{2 \cdot (\pi - \alpha)}{\pi} & \text{for } \alpha \in [\frac{\pi}{2}, \pi) \end{cases} \quad (1)$$

for $r \in [r_1, r_2]$,

where (x, y, z) is the point of the surface, and α is the radian in the $x-y$ plane in the wheel, and r is the distance to the z -axis. It is for the supporting structure when $r \in [0, r_1]$.

The rotating wheel filter is made of a thin plate of plexiglass (PMMA 340×340×20 mm) and has a periodic structure of very fine and precise slopes (Figs. 1 and 2). They have to be manufactured to their desired form with a mechanical precision of about 5–10 μm . Continuous fluid cooling and fixing of the rotating wheel filter on a vacuum table improves the

cutting quality. Figs. 1 and 2 show the design and the accurate structure. Optimization of the shape of the slope is described in section 2.5.

2.2 Wheel movement and dosimetric measurements

The wheel is rotating at 20 rounds per minute (rpm) while the beam penetrates the region of variation in the z -axial direction. And the Bragg peak is moving in the SOBP region at the varying speed to form a wide SOBP.

Depth dose measurements is performed with the ionization chambers (PTW/Markus) irradiated in water to determine the shape of the depth dose curves for the 90 MeV/nucleon unmodulated and modulated $^{12}\text{C}^{6+}$ beam.

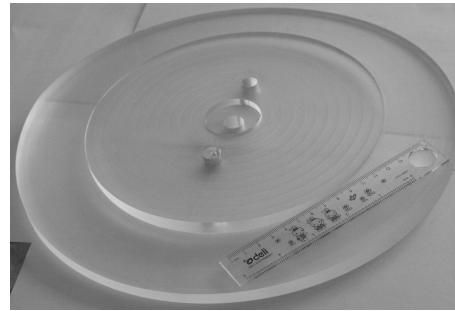


Fig. 1. Rotating wheel filter. The wheel is rotating while the beam penetrates the varying region in the z -axial direction. And the Bragg peak is moving in the SOBP region in the varying speed to form a wide SOBP.

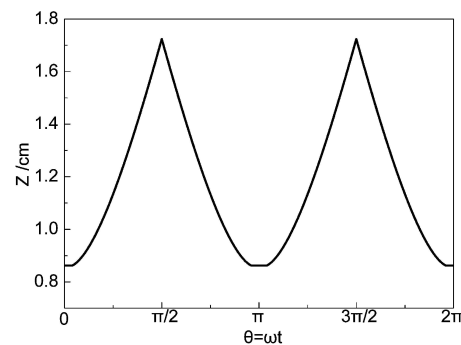


Fig. 2. Cross section of the rotating wheel filter. The wheel is used to obtain 1 cm SOBP for carbon ion therapy.

2.3 Cell survival and biological dose

Along the track of a carbon-ion beam, LET values are changing from around 10 keV/ μm to a few hundred keV/ μm . This has a significant impact on the cell survival and has to be taken into account when

carbon beams of different energies are combined. The method used for estimating the relative cell survival is the linear-quadratic model,

$$SF = \exp(-\alpha D - \beta D^2). \quad (2)$$

The variables— α and β —depend on the dose-averaged LET which varies as a function of depth for charged irradiation.

In this work, we used the D_{10} (dose which would reduce cell survival to 10%) obtained from cell survival experiments on V79 cells irradiated at different LET in the carbon ion beam at The Heavy Ion Medical Accelerator in Chiba (HIMAC)^[1].

The RBE is obtained from the ratio between the doses required to obtain a desired level of cell killing of a reference radiation quality (X-rays),

$$\begin{aligned} \text{RBE}(\text{LET}, sl) = \\ \frac{D_{\text{X-Ray}}(\alpha_{\text{X-Ray}}, \beta_{\text{X-Ray}}, sl)}{D_{\text{carbon-ion}}(\alpha_{\text{carbon-ion}}(\text{LET}), \beta_{\text{carbon-ion}}(\text{LET}), sl)}. \end{aligned} \quad (3)$$

The RBE thus depends on the LET and the choice of the survival level (sl). $D_{\text{X-Ray}}(sl = 10\%)$ and $D_{\text{carbon-ion}}(sl = 10\%)$ are obtained from Furusawa group's report^[1]. The biological dose as a function of the LET and the survival level follows straightforward:

$$D_{\text{bio}}(x, \text{LET}, sl) = \text{RBE}(\text{LET}, sl) g D_{\text{Phys}}(x, \text{LET}, sl), \quad (4)$$

where $D_{\text{bio}}(x, \text{LET}, sl)$ and $D_{\text{Phys}}(x, \text{LET}, sl)$ represent the biology dose and physical dose at the survival level (sl) and at position x , when the LET is LET.

2.4 Bragg peak movement and biological dose distribution

The beam penetrates the wheel in the z-axis direction (Fig. 1) while the wheel is rotated at a constant speed. The Bragg peak will be oscillated in the section of the SOBP. During a quarter of the wheel rotation, the physical LET distribution can be described by the following function,

$$D_{\text{SOBP}}^{\text{Phys}}(x) = \int_0^T F(t) \cdot D d_{\text{phys}}[x + \int_0^t v(t) dt] dt, \quad (5)$$

where $v(t)$ represents the speed of the Bragg peak movement at time t , $D_{\text{SOBP}}^{\text{Phys}}(x)$ represents the physical dose distribution in depth after SOBP performed, $F(t)$ represents the ion flux at the time t , $D d_{\text{phys}}(x)$ represents the pristine physical dose distribution.

$F(t)$ can be modulated to a constant on the Heavy Ion Research Facility in Lanzhou (HIRFL). So Eq. (6) can be get from Eq. (5),

$$D_{\text{SOBP}}^{\text{Phys}}(x) = F(t) \cdot \int_0^T D d_{\text{phys}}[x + \int_0^t v(t) dt] dt. \quad (6)$$

And the biology dose distribution can be described by the following function basing on the Eq. (4),

$$\begin{aligned} D_{\text{SOBP}}^{\text{bio}}(x) = \int_0^T \text{RBE}(\text{LET}_{\text{phys}}[x + \int_0^t v(t) dt]) \cdot F(t) \\ \cdot D d_{\text{phys}}[x + \int_0^t v(t) dt] dt = F(t) \cdot \int_0^T \text{RBE}(\text{LET}_{\text{phys}}[x + \\ \int_0^t v(t) dt]) \cdot D d_{\text{phys}}[x + \int_0^t v(t) dt] dt, \end{aligned} \quad (7)$$

where $D_{\text{SOBP}}^{\text{bio}}(x)$ represents the biology dose distribution in depth after SOBP performed.

2.5 Resolve of Bragg peak movement

To achieve the biological uniform dose distribution, a function of Bragg peak movement is presented,

$$\begin{aligned} \int_0^t v(t) dt = \\ \text{Broad} \cdot \frac{a_1 \cdot t + t^{1.5} + a_2 \cdot t^2 + a_3 \cdot t^3 + \dots + a_n \cdot t^n}{a_1 \cdot T + T^{1.5} + a_2 \cdot T^2 + a_3 \cdot T^3 + \dots + a_n \cdot T^n} \end{aligned} \quad (8)$$

for $t \in [0, T]$

It is the distance function of the Bragg movement at the time t , here, broad is the SOBP broad.

So the rotating wheel can be designed by minimizing the following function,

$$\begin{aligned} \text{Relstdev} \left(\begin{array}{c} a_i \\ i = 1, 2, \dots, n \end{array} \right) = \\ \frac{\left\{ \frac{1}{m-1} \sum_1^m [D_{\text{SOBP}^{\text{bio}}}(x_i) - \frac{1}{m} \sum_1^m D_{\text{SOBP}^{\text{bio}}}(x_i)]^2 \right\}^{\frac{1}{2}}}{\frac{1}{m} \sum_1^m D_{\text{SOBP}^{\text{bio}}}(x_i)}, \end{aligned} \quad (9)$$

where $\text{Relstdev}(a_i, i = 1, 2, \dots, n)$ represents the relative standard deviation of the section of SOBP, m represents the number of the points selected from the section of SOBP, and x_i represents the position in the section of the SOBP. We have developed a computer program to determine the movement of the Bragg peak to yield a flat-topped SOBP. The coefficients ($a_i, i = 1, 2, \dots, n$) are obtained with Monte Carlo method (Fig. 3).

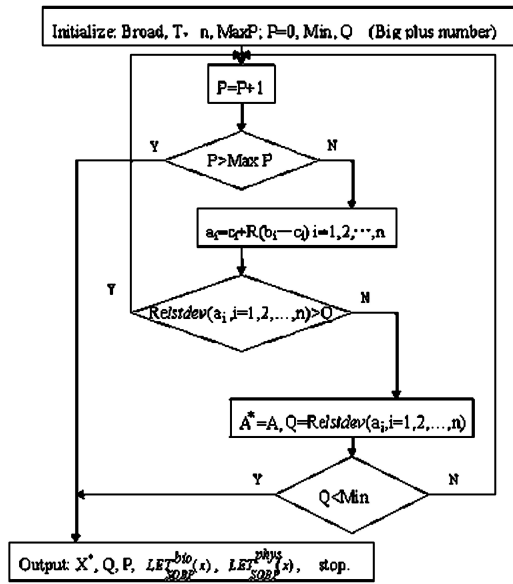


Fig. 3. Program flow graph of Monte Carlo method. Monte Carlo method is a direction solution. Some random experiment points are selected from an area, $\{(a_1, a_2, \dots, a_n) | a_i \in (c_i, b_i), i = 1, 2, \dots, n\}$. Then, the least point is obtained from these random experiment points. The solution is the least point.

Monte Carlo method is a direction solution. Some random experiment points are selected from an area, $\{(a_1, a_2, \dots, a_n) | a_i \in (c_i, b_i), i = 1, 2, \dots, n\}$. Then, the least point is obtained from these random experiment points. a_i is obtained by the following method, $a_i = c_i + R(b_i - c_i), i = 1, 2, \dots, n$, where R is a random number which obeys to the uniform $[0, 1]$ distribution.

n : the dimension number of the experiment point
 P : the total number of the experiment points;
 $\text{Max } P$: the number of the maximum experiment points;
 Broad : the broad of the SOBP;
 A : the experiment point (a_1, a_2, \dots, a_n) ;
 A^* : the iterative optimization point;
 Q : the minimum value of $\text{Relstdev}(a_i, i = 1, 2, \dots, n)$ in the iterating process, its initial value is the big number that can be given by the computer.

In the treatment planning, incident particles are modeled to form a parallel broad beam with the physical depth-dose distribution given by the one-dimensional HIBRAC code^[6] considering up to the tertiary projectile fragmentation in water. So the data of Bragg curves, which are used for this program, are calculated in a water target with the Hibrac code and measured in water with PTW/Markus. The data of RBE are obtained from Furusawa group's report^[1].

The entire displaced Bragg curve is determined from the pristine Bragg curve using quadratic Lagrangian interpolation. And the RBE curve is determined by the same interpolation.

3 Result

We have applied the method for many treatment depths with satisfactory results. We will present an examples here as the illustration.

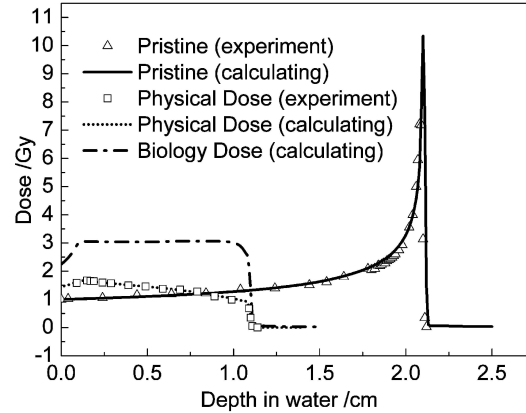


Fig. 4. Depth dose distributions. Pristine (experiment) and Pristine (calculating) represent the experimental result of the pristine Bragg curves measured by PTW/Markus and calculated by Hibragg program respectively. Physical dose (experiment) and physical dose (calculating) represent the SOBP physical dose distributions measured by PTW/Markus and calculated by the Hibragg program respectively. And Biology dose represents the RBE dose distribution calculated through the Pristine (experiment). The results are normalized to the entrance energy deposition. Biology dose (calculating) shows the 1 cm wide SOBP for 90 MeV/nucleon $^{12}\text{C}^{6+}$, and it is flat to $\pm 0.6\%$ over the SOBP region.

An example of a calculation is shown in figure 4 for HIRFL. For this particular case, the energy of the incident carbon ion ($^{12}\text{C}^{6+}$) beam is 90 MeV/nucleon, and the initiation parameters are initialized, $\text{Broad}=1, T=1, n=3, \text{Max } P=10000, \text{Min}=0.006, Q=1$. The results are normalized to the entrance energy deposition. The biology dose (calculating according to the data of the pristine Bragg curve measured by PTW/Markus) (Fig. 4) is flat to $\pm 0.6\%$ over the SOBP region. The physical dose peak and the pristine peak are shown for reference. And the movement coefficient of the Bragg

peak is the following, $a_1 = -0.285958$, $a_2 = 0.0451064$, $a_3 = -0.092349$.

So the rotating wheel filter (Fig. 1) can be designed basing on Eq. (1). The cross section of the rotating wheel filter made of Plexiglas is shown in Fig. 2 for 90 MeV/nucleon, which provide the continuous variation of the depth of penetration. Here $r_1=11$ cm, $r_2=16$ cm, $C=0.862$ cm, $C_m=0.862$ cm, of which r_1 and r_2 are determined by the terminal for cancer therapy of HIRFL, C and C_m are determined by the manufacturing condition and material of Plexiglas respectively.

4 Discussion

Pshenichnov et al applied a Monte Carlo simulation to heavy ion beams and showed its effectiveness for calculating accurate physical dose distribution^[7]. However accuracy improvement in the physical dose is not enough for treatment planning because prediction of the biological dose is essential in heavy ion radiotherapy^[8]. Therefore, we have developed

a new design method for the rotating wheel filter considering the RBE. For carbon ions with energy from 80 MeV/nucleon to 250 MeV/nucleon, the design works well. In this study, the data of measurement matches well with the calculating result from Hibragg (Fig. 4). And the biology dose distribution in the SOBP region is flat enough to $\pm 0.6\%$ for the tumor therapy. Although the wheel works well for the stable beam, it dose not agree with the variable intensity beam unless the rotary speed of the wheel was modulated with the beam intensity.

The advantages of the rotating wheel filter design may be summed up as follows, being compact, cheap, and easy to manufacture, and flat enough to form the SOBP region. Usage of these distributions for treatment planning is currently under exploration. This technique may obviously be extended to the range modulation of proton beams.

We express our thanks to the accelerator crew at the HIRFL, National Laboratory of Heavy Ion Accelerator in Lanzhou.

References

- 1 Furusawa Y, Fukutsu K, Aoki M et al. Radiat. Res., 2000, **154**(5): 485–496
- 2 Chu W T, Ludewigt B A, Renner T R. Rev. Sci. Instr., 1993, **64**(8): 2055–2122
- 3 Petti P L, Lyman J T, Castro J R. Med. Phys., 1991, **18**(3): 506–512
- 4 Koehler A M, Schneider R J, Sisterson J M. Nucl. Instrum. Methods, 1975, **131**(3): 437–440
- 5 Jongen Y, Beeckman W, Laisne A. Development of a low-cost compact cyclotron system for proton therapy. In: Proceedings of the NIRS international workshop on Heavy Charged Particle Therapy and Related subjects. Chiba. 1991. 189–200
- 6 Sihver L, Schardt D, Kanai T. Jpn. J. Med. Phys., 1998, **18**(1): 1–21
- 7 Pshenichnov I, Mishustin I, Greiner W. Phys. Med. Biol., 2005, **50**(23): 5493–5507
- 8 Kase Y, Kanematsu N, Kanai T, Matsufuji A. Phys. Med. Biol., 2006, **51**: N467–475